ELSEVIER

Thermochimica Acta 299 (1997) 59–65

thermochimica
acta

Activation energies for the desorption of neutral molecules and positive ions from alkali-halide layers heated on a metal surface

Hiroyuki Kawano*, Yongfa Zhu[1], Susumu Kamidoi, Hironari Shimizu, Masayuki Udaka

Department of Chemistry, Faculty of Science, Ehime University, Matsuyama, 790-77, Japan

Abstract

To determine the activation energies (E^+ and E^0) and the frequency factors (ν^+ and ν^0) for thermal positive-ionic and neutral desorption from an ionic crystalline surface in high vacuum, a thin film ($\theta_0 \approx 70$–1400 molecular layers composed of 2.5–50 nmol) of alkali halide (MX) deposited on a platinum plate (ca. 0.03 cm^2) was heated up to ca. 1500 K at a constant rate ($\beta \approx 2$–80 K s^{-1}), and the absolute desorption rates of the ions (M^+) and neutral molecules (MX^0) were simultaneously measured by using our thermal ionization type dual-ion source system operated by a temperature-programmed desorption method. This system had so high a detection sensitivity that even desorption rates of ca. 10^5 ions s^{-1} and ca. 10^{10} molecules s^{-1} were readily measured with reasonable accuracy. In each of the desorption spectra obtained with sodium halides, NaX^0 and Na^+ showed single sharp peaks at low and high temperatures corresponding to ca. 40% and < 0.4% of θ_0, respectively. Theoretical analysis of the relation between β and each desorption peak-appearance temperature ($T_p \approx 700$–1300 K) furnished the following results; NaCl ($E^0 = 193$–176 and $E^+ = 290$ kJ mol^{-1}; $\nu^0 = 10^{10.7}$ and $\nu^+ = 10^{11.6}$–$10^{12.3}$ s^{-1}), NaBr (112 and 257; $10^{6.7}$ and $10^{11.0}$), NaI (139 and 234; $10^{9.4}$ and $10^{9.9}$). RbCl, having two peaks of Rb^+ alone at adjacent (a) low, and (b) high temperatures, afforded the data; (154 and (a) 239, (b) 205; $10^{9.9}$ and (a) $10^{11.7}$, (b) $10^{9.1}$), while LiCl with two peaks of both $LiCl^0$ and Li^+ yielded ((a) 145 and 291, (b) 277 and 234; (a) $10^{9.6}$ and $10^{12.6}$, (b) $10^{11.7}$ and $10^{9.0}$), respectively. Physico-chemical analysis of these data supplied a substantial clue to the ionic and neutral desorption processes and mechanisms.

Keywords: Activation energy; Alkali-halide layers; Frequency factor; Ionic and neutral desorption rates; Thermal desorption processes

1. Introduction

When a sample of an ionic crystal such as alkali halide (MX), deposited on a substrate metal surface (SMS), is heated to a high temperature (T) – above ca. 700 K – in vacuum, positive or negative ions (M^+ or X^-) are usually desorbed together with neutral molecules (MX^0) without including an appreciable amount of neutral atoms (M^0 and X^0). This phenomenon is called 'dissociative self-surface ionization' and has long been widely utilized as a rather convenient method to generate ion beams, to prepare and control a thin film, to determine relative abundances of stable or unstable isotopes, to analyze impurities or contaminants, and so on [1]. The desorption processes themselves, however, have not fully been understood to-date. To clarify the processes and physico-chemical factors governing desorption, we have developed a convenient method using our dual-ion source (DIS) system operated by a temperature-programmed desorption (TPD) technique. With this apparatus, it has become very easy to simultaneously measure ionic

---

*Corresponding author. E-mail: kawano@dpc.ehime-u.ac.jp

[1] On leave from the Department of Chemistry, Tsinghua University, Beijing, 100084, P.R. China.

0040-6031/97/$17.00
PII S0040-6031(97)00137-8

and neutral desorption rates ($n^{\pm}$ and n^{0}) as functions of both, sample temperature (T) increasing at a constant rate (β) and mean sample layer thickness (θ) or sample amount (N) remaining on SMS.

This paper summarizes the experimental data on both activation energies (E^{+} and E^{0}) and frequency factors (ν^{+} and ν^{0}) for the desorption of M^{+} and MX^{0}, and also analyzes the data from the viewpoints of chemical thermodynamics and surface science.

2. Experimental

The ion-source system is schematically shown in Fig. 1. The experimental procedure used by us may be outlined as follows. With a microsyringe, 0.50 µl of an aqueous solution (0.005–0.1 mol l^{-1}) of MX is deposited onto a platinum plate (F_1, 0.034 cm^2) and dried at room temperature to prepare a thin film of 70–1400 molecular layers. In a readily attainable high-vacuum ($\approx 10^{-4}$ Pa), F_1 is heated by a coiled tungsten or rhenium heater (H) up to ca. 1500 K at a constant rate (β). The sample temperature (T) is measured with a calibrated Alumel-Chromel thermocouple (A). Neutral molecules (MX^{0}) desorbed from F_1 are detected with a coiled platinum wire (F_2) heated to 1260 K. The primary and secondary ion currents (i_1^{+} and i_2^{+}) of M^{+}, desorbed from F_1 and F_2 maintained at the bias potentials of +30 and +16 V, are directly collected by respective Faraday cups (C_1 and C_2) since their mutual mixing is prevented by a grid (G) kept at +50 V with respect to the earth. The copper block (B) can be cooled to ca. 0°C by circulating ice water (W) in order to suppress the evaporation of MX deposited gradually onto the cylinder walls during a run. The efficiencies (η^{+} and η^{0}) of the primary ion

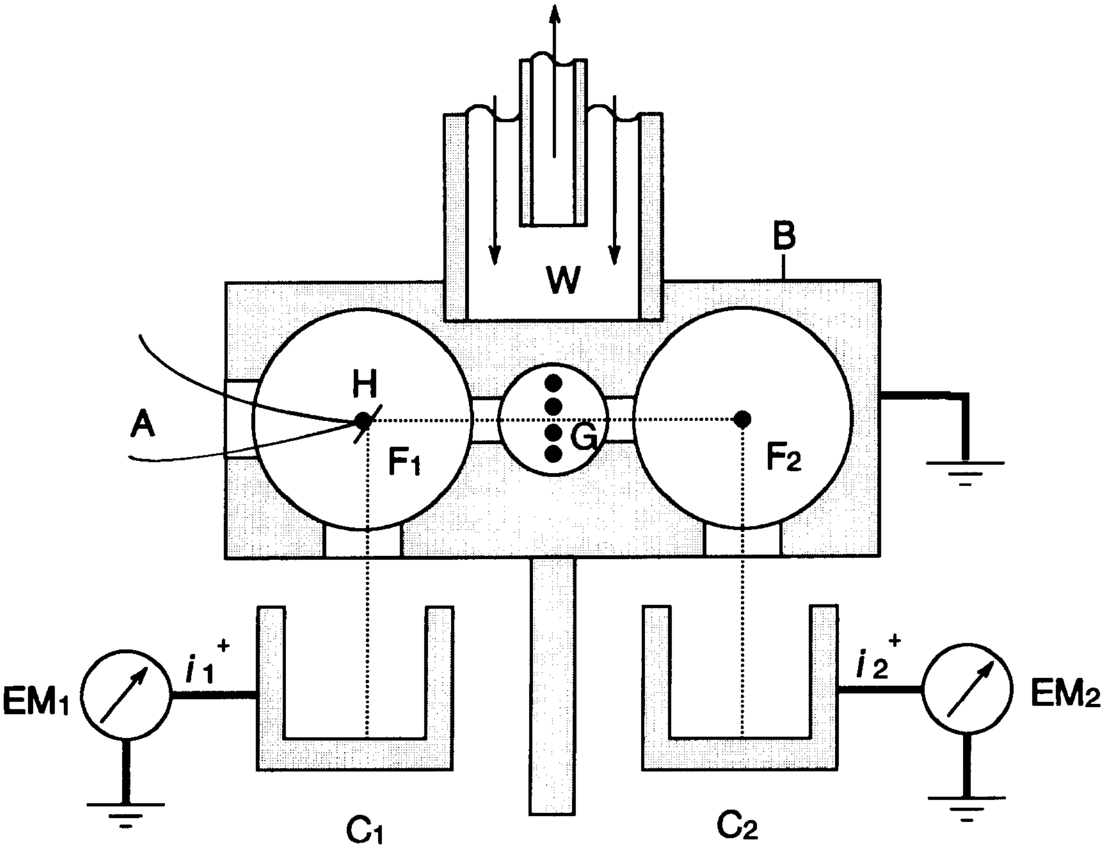

Fig. 1. Schematic diagram of our instrument. See text for the legend.

collection and the neutral molecular detection under the aforementioned conditions are 0.34 ± 0.02 and (3.3 ± 2.3) × 10^{-4}, respectively, as determined by our simple method [2]. The current (i_1^-) of X^- from NaX, RbCl or LiCl is too weak to be detected in the temperature range (< 1000 K), low enough to neglect the thermal electron current compared with i_1^-, in contrast to the case of F^- from LiF or KF [3,4]. The number (N) and mean layer thickness (θ) at a given time (t) or T are evaluated according to Eqs. (7 and 8) described in Ref. [3]. Mass spectrometry of NaCl in a separate experiment indicates that MX^0 and M^+ consist mainly of the monomer of NaCl (> 90%), and the ion of Na^+ (> 99%), respectively.

In this way, our method makes it possible to simultaneously measure both, positive ionic ($n^+ \equiv i_1^+/e\eta^+$) and neutral desorption ($n^0 \equiv i_2^+/e\eta^0$) rates, where e is the elementary electric charge, and also to determine both N and θ as functions of either T or t. It should be noted that $n^+ > 10^5$ ions s^{-1} (10^{-19} mol s^{-1}) and $n^0 > 10^{10}$ molecules s^{-1} (10^{-14} mol s^{-1}) are readily determined since the electrometers (EM_1 and EM_2) have sensitivities of ca. 1×10^{-15} and ca. 1×10^{-13} A div^{-1}, respectively.

3. Results and discussion

A typical spectrum observed with NaCl at $\beta \approx 63$ and 4 K s^{-1} is shown in Fig. 2, where the sample amount (N_0) deposited on F_1 was 2.5 nmol (1.5 × 10^{15} molecules), and hence, the mean layer thickness (θ_0) at the start was evaluated to be ca. 70 molecular layers (ML). The heights of peaks on curves (2) and (2′) are 100 and 10 times, respectively, and hence expressed on scales of 0.01 nA and 0.1 μA, respectively. At β = constant, $NaCl^0$ and Na^+ gave single peaks at both low and high temperatures (T_p^0 and T_p^+), respectively. Each of the temperatures decreased with reduction in β. Similar results were also obtained with NaBr and NaI. With respect to RbCl, on the other hand, two peaks (a and b) are found with Rb^+, as exemplified in Fig. 3. In the case of LiCl, both $LiCl^0$ and Li^+ exhibit two peaks (see Fig. 4).

In this way, both T_p^0 and T_p^+ were measured simultaneously as a function of β, and the data thus obtained were analyzed by the following equation [5]:

$$\ln(T_p^2/\beta) = (E/RT_p) - \ln(\nu R/E) \qquad (1)$$

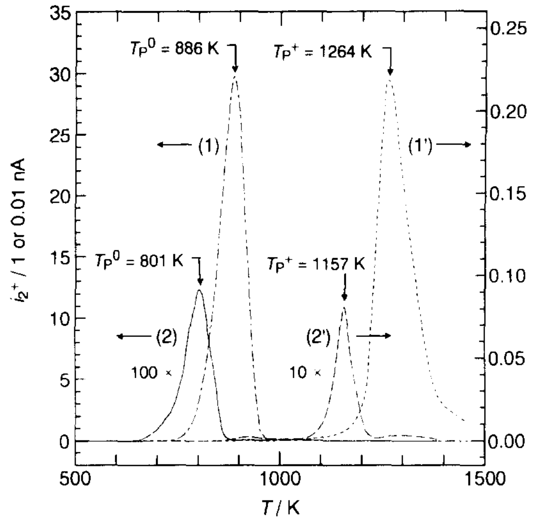

Fig. 2. Neutral and ionic desorption spectrum observed with NaCl (2.5 nmol deposited). Curves (1) and (1′) are obtained with $NaCl^0$ and Na^+, respectively, at $\beta \approx 63$ K s^{-1}, while (2) and (2′) are obtained at $\beta \approx 4$ K s^{-1}. The heights of peaks (2) and (2′) are expressed by the scales of 0.01 nA and 0.1 μA, respectively.

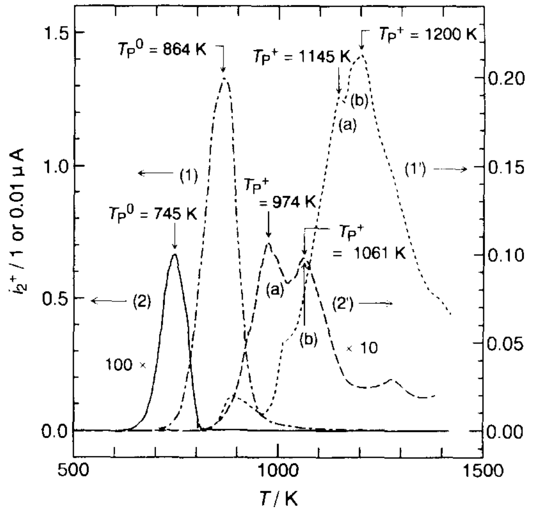

Fig. 3. TPD spectrum achieved with RbCl (2.5 nmol deposited). Curves (1) and (1′) were observed, respectively, with $RbCl^0$ and Rb^+ at $\beta \approx 63$ K s^{-1}, whereas (2) and (2′) were observed at ca. 4 K s^{-1}.

The results achieved with MX^0, Na^+ and M^+ are illustrated in Figs. 5–7, respectively. With each desorbed particle, E and ν determined from the slope and

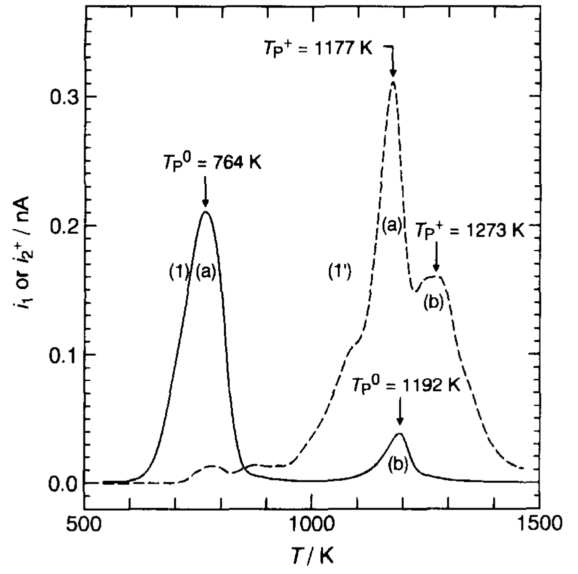

Fig. 4. Desorption spectrum found with LiCl (10 nmol deposited). Curves (1) and (1') correspond to $LiCl^0$ and Li^+, respectively, desorbed by heating at $\beta \approx 7\ K\,s^{-1}$.

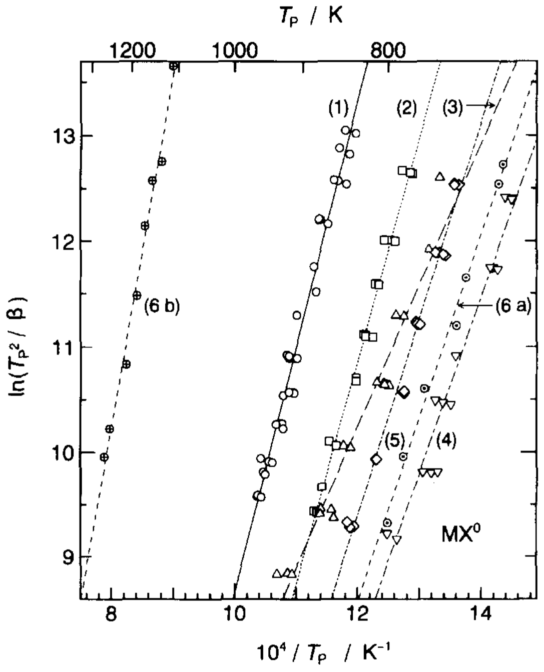

Fig. 5. The reciprocal of the peak appearance temperature (T_p^0) of MX^0 vs. the natural logarithm of $(T_p^0)^2/\beta$, where β ranges from ca. 2 to $80\ K\,s^{-1}$: (1) – NaCl (50 nmol deposited); (2) – NaCl (2.5 nmol); (3) – NaBr (2.5 nmol); (4) – NaI (2.5 nmol); (5) – RbCl (2.5 nmol); and (6a,6b) – LiCl (10 nmol).

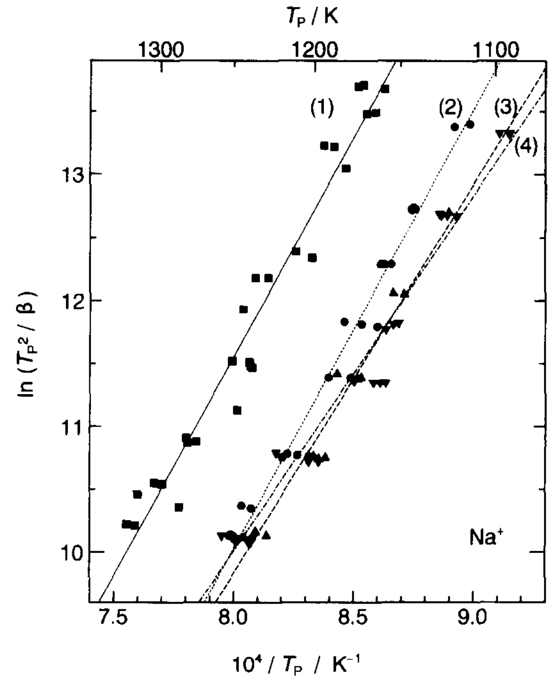

Fig. 6. The reciprocal of T_p^+ for Na^+ from NaX vs. ln $(T_p^+)^2/\beta$ measured with (1) – NaCl (50 nmol deposited), (2) – NaCl (2.5 nmol), (3) – NaBr (2.5 nmol), and (4) – NaI (2.5 nmol).

intercept of each line are summarized in Table 1, indicating that the energies and frequency factors determined with both $NaCl^0$ and Na^+ are nearly independent of θ_0.

Typical results shown in Fig. 8, reveal that T_p^+ corresponds to a very thin film ($\theta < 1$ ML). Hence, it is seen that Rb^+ is directly desorbed from SMS, in contrast to $RbCl^0$ desorbed from its own layers. Also, Na^+ is the result of direct desorption. In this case, E^+ depends generally upon the work function (ϕ) of SMS, in accordance with $E^+ = \varepsilon^0 + I - \phi$ [6]. Here, ε^0 and I are the activation energy for the desorption of M^0 (not MX^0) and the ionization energy of M^0, respectively. Consequently, it may be suggested from the data on E^+ that ϕ of the NaCl/Pt system at $\theta < 1$ ML is smaller by ca. 30 and 50 kJ mol^{-1} than that of the NaBr/Pt and NaI/Pt systems, respectively. It should be noted that surfaces are usually inhomogeneous with respect to ϕ and, hence, M^+ is desorbed predominantly from those active sites having higher values of ϕ [1].

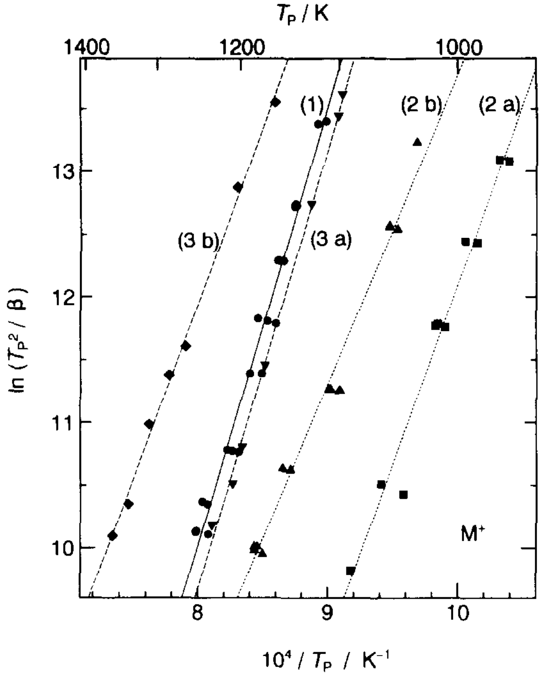

Fig. 7. Comparison of the data on M$^+$ desorbed from (1) – NaCl (2.5 nmol deposited), (2a, 2b) – RbCl (2.5 nmol), and (3a, 3b) – LiCl (10 nmol).

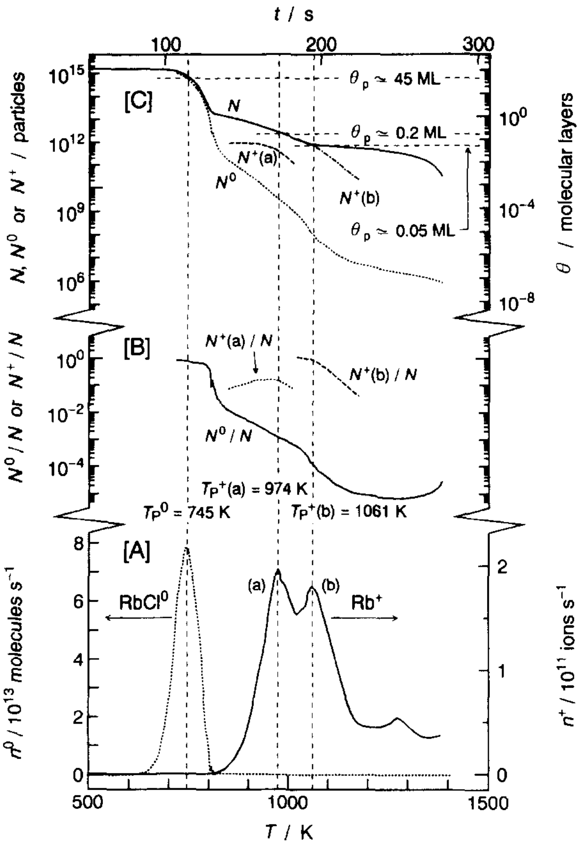

Fig. 8. Typical result achieved with RbCl (2.5 nmol deposited): [A] – TPD spectrum at $\beta = 4$ K s^{-1}; [B] – relative value (N^0/N or N^+/N) participating in the neutral or ionic desorption; and [C] – amount (N, N^0 or N^+) or layer thickness (θ) of the sample present on F$_1$.

The numbers of positive ions (N^+) and neutral molecules (N^0) participating in respective desorptions at any temperature are given [7] by

$$n^{+0} = N^{+0}\nu^{+0}\exp(-E^{+0}/RT) \qquad (2)$$

Therefore, the experimental data on n^{+0} and T, in addition to those on ν^{+0} and E^{+0} listed in Table 1, make it possible to evaluate both N^+ and N^0. A typical result achieved with RbCl ($N_0 = 1.5 \times 10^{15}$ molecules and $\theta_0 = 96$ ML) is illustrated in Fig. 8, yielding the main points as follows.

Table 1
Summary of the desorption parameters determined in the (~700–1300) K range at $\beta \approx 2$–80 K s^{-1}

Sample	N_0/(nmol)	θ_0/(ML) [a]	E^0/(kJ mol^{-1})	ν_0/(s^{-1})	E^+/(kJ mol^{-1})	ν^+/(s^{-1})
NaCl	50	1400	193 ± 13	$10^{10.7\pm0.1}$	289 ± 12	$10^{11.6\pm0.1}$
NaCl	2.5	70	176 ± 6	$10^{10.7\pm0.1}$	290 ± 11	$10^{12.3\pm0.1}$
NaBr	2.5	78	112 ± 6	$10^{6.7\pm0.4}$	257 ± 13	$10^{11.0\pm0.1}$
NaI	2.5	93	139 ± 8	$10^{9.4\pm0.2}$	234 ± 10	$10^{9.9\pm0.1}$
RbCl	2.5	96	154 ± 6	$10^{9.9\pm0.2}$	(a) 239 ± 15	$10^{11.7\pm0.1}$
					(b) 205 ± 8	$10^{9.1\pm0.1}$
LiCl	10	210	(a) 145 ± 6	$10^{9.6\pm0.1}$	(a) 291 ± 6	$10^{12.6\pm0.1}$
			(b) 277 ± 13	$10^{11.7\pm0.1}$	(b) 234 ± 7	$10^{9.0\pm0.1}$

[a] ML=molecular layers.

(1) At $T_\mathrm{p}^0 = 745$ K, for example, the sample amount (N_p) still present on F_1, is ca. 7.2×10^{14} molecules, corresponding to $\theta_\mathrm{p} \approx 45$ ML, while the amount (N_p^0) participating in the neutral deposition is ca. 5.6×10^{14} molecules which is equivalent to ca. 35 ML. Consequently, those molecules included in the upper layers (θ_u^0) of ca. 35 ML (equivalent to ca. 78% of N_p) alone participate in the neutral desorption, and only those (ca. 14% of N_p^0) satisfying $E^0 \geq 154$ kJ mol^{-1} are desorbed as RbCl^0 at the rate (n_p^0) of ca. 7.8×10^{13} molecules s^{-1} at T_p^0.

(2) At $T_\mathrm{p}^+ = 974$ K corresponding to peak (a), for instance, N_p and θ_p are ca. 2.7×10^{12} molecules and 0.2 ML, corresponding to only 0.2% of N_0 and θ_0, respectively, while N_p^+ and θ_p, representing the surface concentration of Rb^+, are ca. 4.0×10^{11} and ca. 0.03 ML, respectively. The value of $N_\mathrm{p}^+/N_\mathrm{p} = 0.15$ suggests that only those particles (Rb^+, Rb and/or RbCl), present on the active sites with higher values of ϕ, participate in the ionic desorption and only those (ca. 50% of N_p^+) having E^+ larger than 239 kJ mol^{-1} are desorbed as Rb^+ at the rate (n_p^+) of ca. 2.0×10^{11} ions s^{-1} at T_p^+. In other words, $N_\mathrm{p}^+/N_\mathrm{p}$ is seen to represent the fractional surface area (F_a) of the active sites over the emitter at T_p^+.

(3) At $T_\mathrm{p}^+ = 1061$ K yielding peak (b), $F_\mathrm{a} \equiv N_\mathrm{p}^+/N_\mathrm{p}$ is 0.86, i.e. larger than 0.15 for peak (a). This result indicates that the surface area having higher work functions facilitates by about six times the desorption of Rb^+ at (b) as compared to that at (a).

In this way, the theoretical analysis is performed with other systems studied at $\beta \approx 4$ K s^{-1}, and the results are summarized in Table 2, affording interesting information as follows.

(1) Irrespective of the value of θ_0 and the species of MX, T_p^0 appears at $\theta_\mathrm{p} \approx \theta_0/2$ and T_p^0 is lower than T_p^+,

Table 2
Summary of the desorption parameters at peak appearance temperatures attained at $\beta \simeq 4$ K s^{-1}

Sample/(nmol)	θ_0/ML [a]	T_p^0/K	N_p/M[b]	θ_p/ML	N_p^0/M	$N_\mathrm{p}^0/N_\mathrm{p}$	θ_u^0/ML	n_p^0/M s^{-1}
NaCl (50)	1400	883	1.2×10^{16}	560	6.6×10^{15}	0.55	300	1.2×10^{15}
NaCl (2.5)	70	801	6.9×10^{14}	32	4.8×10^{14}	0.70	22	7.2×10^{13}
NaBr (2.5)	78	758	5.9×10^{14}	30	5.0×10^{14}	0.85	25	1.1×10^{14}
NaI (2.5)	93	705	6.5×10^{14}	40	6.2×10^{14}	0.95	38	8.7×10^{13}
RbCl (2.5)	96	745	7.2×10^{14}	45	5.6×10^{14}	0.78	35	7.8×10^{13}
LiCl (10)	210	(a) 738	3.2×10^{15}	110	2.5×10^{15}	0.78	86	2.0×10^{14}
		(b) 1136	6.7×10^{14}	23	1.9×10^{14}	0.28	6	5.2×10^{13}

Sample/(nmol)	N_0/M	T_p^+/K	N_p/M	θ_p/ML	N_p^+/ions	$N_\mathrm{p}^+/N_\mathrm{p}$	n_p^+/ions s^{-1}
NaCl (50)	3.0×10^{16}	1238	1.8×10^{13}	0.8	2.6×10^{12}	0.14	6.9×10^{11}
NaCl (2.5)	1.5×10^{15}	1157	5.3×10^{12}	0.3	9.3×10^{11}	0.18	1.5×10^{11}
NaBr (2.5)	1.5×10^{15}	1151	7.5×10^{11}	0.04	3.3×10^{11}	0.44	2.8×10^{11}
NaI (2.5)	1.5×10^{15}	1139	3.2×10^{12}	0.2	1.4×10^{12}	0.44	2.0×10^{11}
RbCl (2.5)	1.5×10^{15}	(a) 974	2.7×10^{12}	0.2	4.0×10^{11}	0.15	2.0×10^{11}
		(b) 1061	8.1×10^{11}	0.05	7.0×10^{11}	0.86	1.8×10^{11}
LiCl (10)	6.0×10^{15}	(a) 1052	1.3×10^{15}	48	1.6×10^{12}	1.1×10^{-3}	1.1×10^{10}
		(b) 1127	7.9×10^{14}	27	1.8×10^{12}	2.3×10^{-3}	1.3×10^{10}

ML[a] = molecular layers.
M[b] = molecules.

indicating that MX^0 is desorbed more readily than M^+. This is also supported by the result that E^0 is much smaller than E^+ in any sample system, except the case of LiCl (b) (see Table 1).

(2) The fraction ($N_p^0/N_p = \theta_u^0/\theta_p$) of the sample molecules, participating in the neutral desorption, is not 100% even at T_p^0, but lies in the range from ca. 30% to 95%. In other words, those molecules forming the lower layers (ca. 70–5%) at T_p^0 have nothing to do with the neutral desorption from the upper layers (ca. 30–95%).

(3) Except in the case of LiCl, T_p^+ appears at $\theta_p < 1$ ML and, hence, M^+ is desorbed from the active sites of the substrate metal (Pt). The fraction ($F_a \equiv N_p^+/N_p$) of the sites at T_p^+ changes from 0.14 up to 0.86 according to the species of MX.

(4) In the case of LiCl, on the other hand, T_p^+ is found at $\theta_p \approx 48$–27 ML, indicating that Li^+ is emitted from the layers of LiCl itself in a similar way as in the case of MF [3,4]. Therefore, the fractional surface area (N_p^+/N_p) from which Li^+ is desorbed is less than 10^{-2}, much smaller than that (10^{-1}) in the other cases mentioned in point (3).

4. Conclusions

The essential points achieved in this work may be summarized as follows:

1. Our dual-ion source system developed for ionic crystalline samples (MX) is very useful for the simultaneous measurements of the absolute (not relative) values of both positive-ionic and neutral desorption rates (n^+ and n^0) of M^+ and MX^0.
2. Operation of the system by a TPD method makes it practical to determine both n^+ and n^0 as a function of T, t or θ.
3. TPD spectra obtained as a function of the heating rate ($\beta \approx 10^0 - 10^2 \mathrm{K\ s^{-1}}$) afford new data on both activation energies (E^+ and E^0) and frequency factors (ν^+ and ν^0) for M^+ and MX^0 (see Table 1).
4. Theoretical analysis of the thermochemical data thus obtained enables us to determine the desorption parameters (N_p, N_p^0, θ_u^0, N_p^+, F_a, etc., see Table 2), which supply us with a substantial clue to the ionic and neutral desorption processes and mechanisms and also to the physico-chemical properties of the respective desorbing surfaces (or sites) of each sample system under study.

Much further work, however, is needed to obtain the thermo-chemical data with many other samples on various substrate metal surfaces (SMS), to determine the work function (ϕ) of the surface of SMS or MX itself during ion desorption, and also to clarify the mechanism of a change in ϕ according to T, θ and/or the species of MX employed.

Acknowledgements

This work was partly supported by a Research Grant (No. 06650041) from the Ministry of Education, Science and Culture and also by a Grant (No. 951118) from the Murata Science Foundation.

References

[1] H. Kawano and F.M. Page, Int. J. Mass Spectrom. Ion Phys., 50 (1983) 1.

[2] H. Kawano, S. Kamidoi and H. Shimizu, Rev. Sci. Instrum., 67 (1996) 1387.

[3] H. Kawano, T. Kenpō and Y. Hidaka, Int. J. Mass Spectrom. Ion. Proc., 67 (1985) 331.

[4] H. Kawano, T. Kenpō, H. Koga, Y. Hidaka and M. Suga, Int J. Mass Spectrom. Ion Phys., 47 (1983) 265.

[5] P.A. Redhead, Vacuum, 12 (1962) 203.

[6] M.D. Scheer, R. Klein and J.D. Mckinley, J. Chem. Phys., 55 (1971) 3577.

[7] H. Kawano, S. Kamidoi, H. Shimizu, K. Ushimaru and H. Asada, Appl. Surf. Sci., 100/101 (1996) 174.